Science of the Total Environment 835 (2022) 155560

Contents lists available at ScienceDirect

Science of the Total Environment

journal homepage: www.elsevier.com/locate/scitotenv

Characterizing solute budgets of a tropical Andean páramo ecosystem

Viviana Arízaga-Idrovo [a], Juan Pesántez [a,*], Christian Birkel [b], Pablo Peña [a], Enma Mora [a], Patricio Crespo [a]

[a] Departamento de Recursos Hídricos y Ciencias Ambientales, Facultad de Ingeniería & Facultad de Ciencias Químicas, Universidad de Cuenca, Cuenca, Ecuador
[b] Department of Geography and Water and Global Change Observatory, University of Costa Rica, San José, Costa Rica

HIGHLIGHTS

- The input-export budgets demonstrated high concentrations of DOC, TNb, and some cations in both rainfall and stream water.
- A minimum number of daily stream water samples is recommended to obtain accurate export rates and avoid underestimations.
- The interpolation method was the most appropriate to calculate solute export rates in the páramo, using high-resolution data.

GRAPHICAL ABSTRACT

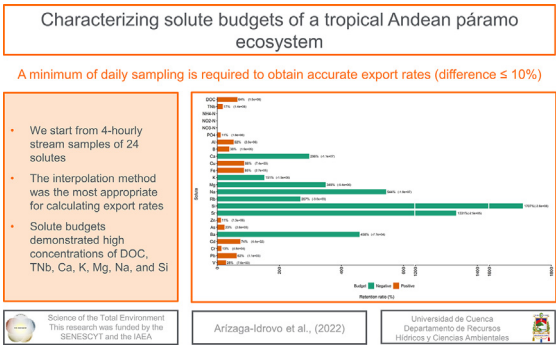

ARTICLE INFO

Editor: Christian Herrera

Keywords:
Solute fluxes
Solute loads
Sampling frequency
Water quality
páramo
Tropics

ABSTRACT

Monitoring solute fluxes in water quality studies is essential to reveal potential ecosystem disturbances, and is particularly important in Andean headwater catchments as they are the main sources of water for downstream populations. However, such studies have mainly focused on organic matter and nutrients, disregarding other solutes that can threaten water quality (e.g. arsenic, lead, calcium or magnesium). Additionally, routine low-resolution (weekly or monthly) sampling schemes may overlook important solute dynamics. Therefore, we collected water samples every four hours for the analysis of twenty-four solutes in a pristine tropical Andean páramo catchment. Solute fluxes were calculated using five different methods. The 4-hourly data set was filtered to test for an optimum sampling frequency without compromising export rates. Based on the available 4-hourly data, the results showed that the interpolation export method was best suited, due to a weak correlation with discharges. Of the twenty-four solutes analyzed, Dissolved Organic Carbon (DOC), Total Nitrogen bound (TNb), Si, Ca, Mg, K, and Na presented the highest input rates (with DOC = 4.167E+08 mEq km^{-2} yr^{-1} and Si = 1.729E+07 mEq km^{-2} yr^{-1}) and export rates (with DOC = 2.686E+08 mEq km^{-2} yr^{-1} and Si = 2.953E+08 mEq km^{-2} yr^{-1}). Moreover, DOC, TNb, NH_4-N, NO_2-N, NO_3-N, PO_4, Al, B, Cu, Fe, Zn, As, Cd, Cr, Pb, and V presented more input than export, while Ca, K, Mg, Na, Rb, Si, Sr, and Ba presented more export than input (geogenic sources). Filtered sampling frequencies demonstrated that a minimum of daily grab samples would be required to obtain reliable export rates with differences consistently below 10%, when compared to the 4-hourly solute export. These findings can be particularly useful for the implementation of long-term monitoring programs at low cost, and they provide high-quality information, for the first time, on biogeochemical budgets in a pristine páramo catchment.

1. Introduction

Quantification of solute fluxes in headwater catchments is essential to assess the water quality of downstream receiving bodies. Solute budget calculations in small catchments are useful as they can provide information about natural or anthropogenic alterations (e.g., land-use changes, extreme

* Corresponding author.
E-mail address: juanp.pesantezv@ucuenca.edu.ec (J. Pesántez).

http://dx.doi.org/10.1016/j.scitotenv.2022.155560
Received 4 January 2022; Received in revised form 19 April 2022; Accepted 23 April 2022
Available online 27 April 2022

rainfall, or atmospheric deposition effects on nutrient cycling and stream chemistry) in the whole ecosystem (McDowell and Asbury, 1994). Nonetheless, there have been no thorough stream solute studies in the Andean páramo or other relatively undisturbed tropical alpine ecosystems. Despite their importance as water towers that provide vital resources for downstream ecosystems and societies in terms of water quantity and quality (Immerzeel et al., 2019), research on these ecosystems has mainly been focused on water quantity (Buytaert and De Bièvre, 2012; Crespo et al., 2011), with little attention to water quality (Correa et al., 2017). Therefore, there is little scientific evidence to examine the assumption of clean waters originating from páramo ecosystems. There has been a lack of research on input, export, and solute budgets, and the factors controlling their dynamics in the Andean páramo.

The main challenge when addressing solute budgets is the measurement of continuous and, to the extent feasible, simultaneous solute concentrations, together with continuous discharge measurements in order to calculate export rates. Discharge values are generally recorded continuously whereas stream grab samples are taken discretely and at different time resolutions. To assess this issue, several methods have been established to estimate solute concentrations. For instance, Walling and Webb (1985) tested different average concentration estimators weighted by the discharge. On the other hand, Johnson (1979), proposed using regression models in order to estimate solute concentrations every time a discharge measurement is available. Furthermore, Schleppi et al. (2006), interpolated solute concentrations between measurements. However, the accuracy and precision of these methods will depend on the correlations between concentrations and discharges. Therefore, the export rates may be biased by the method used for calculation (Dann et al., 1986).

Another difficulty in quantifying export rates is the need for a sampling frequency that covers the entire range of flows (Johnson, 1979). This can be particularly important in small catchments that are highly responsive to rainfall. However, most sample collections are based on a fixed schedule, generally representing base flow conditions (Shanley et al., 2011). High-frequency water quality monitoring is rather uncommon because of the high analytical costs and the sampling constraints in remote locations (Pesántez et al., 2021). Monitoring schemes in export studies generally involve weekly, biweekly or even less frequent sampling resolutions, resulting in the under-representation of high flow samples (Kirchner et al., 2004; Moatar et al., 2012). Therefore, export rates could be significantly under- or overestimated, especially if solute concentrations exhibit large variability under different flow rates (Swistock et al., 1997). This, in turn, generates uncertain solute budgets. As a result, high-frequency measurements have the potential to provide more representative and accurate export rates.

In terms of water quality, most studies have focused on organic matter and nutrients, such as carbon, nitrogen, and phosphorus (e.g., Kortelainen et al., 2006; Ma et al., 2018; Möller et al., 2005; Tang et al., 2008; Vuorenmaa et al., 2002). Other researchers have also studied major cation export such as calcium, potassium, magnesium, and sodium (e.g., Germer et al., 2009; Piazza et al., 2018; Salmon et al., 2001). In the tropics, some studies have monitored element cycling (e.g., Borbor-Cordova et al., 2006; Bücker et al., 2011; Finér et al., 2004; Sánchez-Murillo et al., 2019; Shanley et al., 2011), including nutrients and some cations as well. However, trace metals and other important chemical elements from an environmental and public health perspective (e.g., drinking water, crops irrigation, animal watering troughs) have not been considered, and in most cases only low-frequency sampling was employed in the studies.

In this sense, the objectives of this study are to:

(i) calculate the rainfall input of organic matter, nutrients, cations, and heavy metals in a pristine tropical Andean páramo catchment and test different commonly used methods for export quantification with high-frequency (4-hourly) data;
(ii) filter the high-resolution data and recalculate the export rates in order to obtain an optimum sampling frequency for each solute and evaluate whether or not the sampling hour (i.e., the time of day) has an effect on the export rates; and
(iii) calculate solute budgets and solute retention ratios with export rates at a 4-hourly resolution, compared to the filtered data sets, as an indicator of solute budget uncertainty.

2. Materials and methods

2.1. Study area

The study was conducted in a small (3.28 km^2) catchment within the Zhurucay Ecohydrological Observatory (ZEO), located in the high Andes of southern Ecuador (elevations between 3200 and 3900 m.a.s.l.), that drains into the Pacific Ocean to the west (Fig. 1). The broader ZEO is an experimental páramo catchment that is extensively monitored for hydrometric, meteorological, and water quality data (Mosquera et al., 2016). The catchment in this study is representative of the broader ZEO, with similar hydrogeochemical processes and geomorphological features to other areas within the ZEO (Correa et al., 2019).

The main soil types within the ZEO are Andosols and Histosols, with 74% Andosols and 22% Histosols in the study catchment (Mosquera et al., 2015; Soil Survey Staff, 2003). These soil types are characterized by their high organic matter content (commonly around 35%) and high water retention capacity (Buytaert et al., 2007; Quichimbo et al., 2012). The vegetation is typical for the páramo ecosystem, with tussock grasses covering the Andosols on the hillslopes and cushion plants covering the Histosols in the valley bottoms.

The geology predominantly corresponds to the Quimsacocha Formation (56%), which consists of basalt flows with plagioclases, feldspars, and andesitic pyroclastic deposits (Pratt et al., 1997), and the Turi Formation (31%), that is composed of volcanic breccia, conglomerates, and fluvial sands (Coltorti and Ollier, 2000). Both Formations correspond to the late Miocene Epoch. Lastly, the catchment also contains Quaternary Formations (13%) that were deposited during the glacial activity of the Last Ice Age (Hungerbühler et al., 2002).

The mean annual air temperature is 6 °C and the relative humidity is high at around 91% throughout the year (Córdova et al., 2015). Temperature and precipitation are characterized by low seasonality with an annual average of 1345 mm at 3780 m.a.s.l. (Padrón et al., 2015). Precipitation is homogeneously distributed in space and time over the study area, with no bias and low mean daily precipitation errors, as evaluated via a dense network of rain gauges (Lazo et al., 2019; Seminario, 2016). Mosquera et al. (2015) determined an average annual discharge of 786 mm, with a runoff coefficient of 0.63. Runoff is mainly generated from the Histosols, with significant influences of pre-event water all year round (Correa et al., 2017).

2.2. Hydrometric data

Rainfall was measured with a Texas Electronics tipping-bucket rain gauge (TR-525 M, Dallas, TX, USA) with 0.1 mm resolution and ± 1% accuracy. Spatial rainfall in páramo ecosystems is well represented with one rainfall station within distances of less than 4 km (Buytaert et al., 2006a, 2006b, 2006c). Additionally, the rain gauge, located in the mid-upper part of the catchment, was consistent with the streamflow response (Sucozhañay and Célleri, 2018).

Stream water level measurements were recorded every 5 min through an INW (AquiStar CT2X, Kirkland, WA, USA) pressure transducer sensor with ±0.06% accuracy that was installed in a combined rectangular-V-notch weir at the outlet (Fig. 1). The Kindsvater-Shen equation was applied to transform the water-level data into flow rates (United States Bureau of Reclamation, 2001). Finally, the rating curve was regularly calibrated with salt-dilution streamflow measurements.

2.3. Water quality monitoring and sampling

The monitoring campaign was conducted from April 2018 to March 2019. Rainfall was accumulated in 1000 mL glass bottles to analyze nutrients and in high-density polyethylene (HDPE) bottles to analyze cations

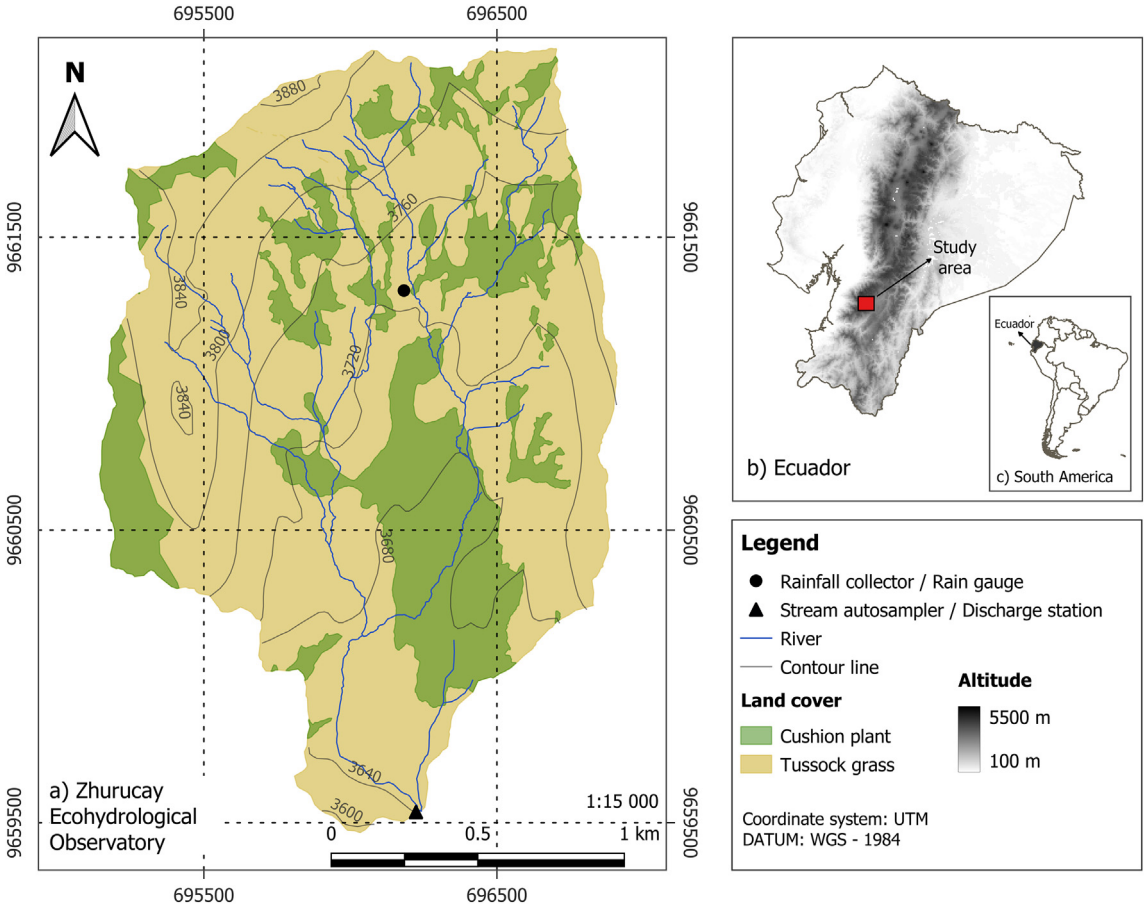

Fig. 1. Study area (a), and location of the Zhurucay Ecohydrological Observatory (ZEO), (b) and (c).

and heavy metals. The bottles were located right next to the rain gauge. Circular funnels with a 16 cm diameter were connected to the bottles and plastic spheres (ping-pong balls) were placed inside to prevent evaporation and contamination. Furthermore, the bottles were wrapped in aluminum foil to reduce the effect of radiation. Bulk rain samples were collected once or twice per week, depending on rainfall occurrence. After sampling, collection bottles were cleaned with Type I distilled water to avoid sample contamination, sediments and algae residues. On the other hand, stream grab samples were collected every four hours using a Campbell Scientific automatic sampler (PVS4100D, Logan, UT, USA).

Three replicate samples were collected, because the preparation of the bottles and the conservation of the samples depends on the solute to be analyzed. Samples were collected in 100 mL HDPE bottles. First, filtered samples (S1) were analyzed for Dissolved Organic Carbon (DOC). Second, unfiltered samples (S2) were analyzed for Total Nitrogen bound (TNb), NH_4-N, NO_2-N, NO_3-N, and PO_4 (nutrients). Prior to sampling, S1 and S2 bottles were washed with Type II and Type I distilled water. Third, additional filtered samples (S3) were analyzed for Al, B, Ca, Cu, Fe, K, Mg, Na, Rb, Si, Sr, Zn, As, Ba, Cd, Cr, Pb, and V (cations and heavy metals). Prior to sampling, S3 bottles were washed with acid-washing equipment (traceClean, Milestone, USA) using ultrapurified nitric acid (HNO_3). Moreover, all bottles were rinsed with streamwater to further homogenize them. S1 and S3 samples were filtered in situ through 0.45 μm polypropylene single-use syringe membrane filters (Puradisc 25 PP Whatman Inc., Clifton, NJ, USA). S1 and S2 sample groups were analyzed the day after collection. If the analysis could not be conducted the day after collection, the samples were stored at −4 °C for no more than one month prior to analysis. S3 samples were immediately acidified with HNO_3 (6%) to avoid trace metal precipitation and adsorption, and analyses were conducted within two months of collection.

2.4. Laboratory analysis

DOC and TNb were analyzed with a liquid sample analyzer (elementar vario TOC cube, Langenselbold, DE) with detection limits of 0.006 mg L^{-1} for DOC and 0.003 mg L^{-1} for TNb. The other nutrients (NH_4-N, NO_2-N, NO_3-N, and PO_4) were analyzed with a segmented flow analyzer (OI Analytical, TX, USA), and the detection limits were 0.003 mg L^{-1} for NH_4-N, 0.0005 mg L^{-1} for NO_2-N and NO_3-N, and 0.001 mg L^{-1} for PO_4. On the other hand, Inductively Coupled Plasma Mass Spectrometry (ICP-MS) (Perkin Elmer, Waltham, MA, USA) was used to determine concentrations of cations and heavy metals (Al, B, Ca, Cu, Fe, K, Mg, Na, Rb, Si, Sr, Zn, As, Ba, Cd, Cr, Pb, and V).

For the TOC cube, Sigma Aldrich (P1088, S5506) (Darmstadt, DE) and VWR Analytical (ACS) (Radnor, PA, USA) standards were used. The standards were Potassium hydrogen phthalate BioXtra ≥99.95% (Sigma Aldrich, MO) for TOC, and Sodium Nitrate ReagentPlus ≥99.0% (Sigma Aldrich, MO) and Ammonium Chloride ≥99.95% (VWR Analytical, PA) for TNb. Six standards were used to build the calibration curve for the TOC cube. For the OI Analytical, a Segmented Flow Analysis (SFA) methodology was conducted, as recommended in United States Environmental Protection Agency (USEPA) guidelines. Certified reference material (ISO 9001 registered and ISO 17025 accredited) (IV ICP-MS 71A, CCS 4, CCS 6, CGSI1, CMS 1) by Inorganic Ventures (Christiansburg, VA, USA) was used to control the quality of the ICP-MS measurements. A minimum of six weight/weight dilutions of the reference material and Type I distilled water were prepared and five calibration curves were constructed for the ICP-MS. A Pearson coefficient of 0.999 was considered for all calibration curves to guarantee accuracy. Every value corresponds to the mean of three consecutive measurements.

2.5. Concentration–discharge relationships

We classified storm events according to dilution, mobilization, or chemostatic behavior to better understand solute dynamics. Logarithmic concentration-discharge scatter plots were constructed to classify the solute dynamics, with the slope of the concentration-discharge relationships indicating the class of solute dynamics: A negative sign indicates dilution, a positive sign indicates mobilization, and where the slope is close to zero, chemostatic behavior can be expected (Godsey et al., 2009; Moatar et al., 2012).

Dilution implies a depletion of the solute concentration with increasing discharge, whereas mobilization behavior results in an increased solute concentration as the discharge increases. Chemostatic behavior suggests only small solute variations across a wide range of discharges (Knapp et al., 2020).

The scatter plots used four selected events to illustrate solute dynamics, with two events from the wetter period and two from the drier period. The events were selected with the Peak Over Threshold method and multipeak events were subdivided. This method involves selecting all peak discharges that exceed a defined threshold in order to select single hydrological events. The 30th percentile of the discharge range (baseflow rate) was used as a threshold (Mosquera et al., 2015). The procedure was performed with the POT R package (Ribatet and Dutang, 2018).

2.6. Input and export analysis

2.6.1. Rainfall inputs

Solute concentrations from the bulk rain samples were weighted by the rain gauge measurements at the time of collection to obtain a volume-weighted mean concentration (VWMC) (Eq. (1)). The VWMC was then multiplied by the amount of total rainfall in the catchment within the study period to quantify solute input (Eq. (2)).

$$VWMC = \frac{\Sigma\, C_i P_i}{\Sigma P_i} \tag{1}$$

$$Input = VWMC * Annual\ rainfall \tag{2}$$

where, C_i = measured concentration and P_i = accumulated rainfall at the time of collection.

2.6.2. Export rates

Usually stream grab samples are collected at a much lower frequency than discharge measurements and we tested five commonly used methods in this study.

- *Method 1* (M1) used the grab samples to calculate a mean concentration independently of the discharge (Eq. (3)).
- *Method 2* (M2) estimated a mean solute concentration by weighting the concentrations by an average discharge, which was calculated for every four hours using the 5-min data (Eq. (4)).
- *Method 3* (M3) weighted the concentrations by the instantaneous discharge at sampling time (Eq. (5)), commonly known as the flow-weighted mean concentration (FWMC). In the same way as the input, the export rates for this method were calculated as the multiplication of these mean concentrations by the total specific discharge within the study period (Eq. (6)).

$$C = \frac{\Sigma\, C_i}{n} \tag{3}$$

$$C = \frac{\Sigma\, C_i\, \overline{Q}_i}{\sum \overline{Q}_i} \tag{4}$$

$$FWMC = \frac{\Sigma\, C_i Q_i}{\Sigma\, Q_i} \tag{5}$$

$$Export = \overline{C} * Annual\ discharge \tag{6}$$

where, C = estimated average concentration, C_i = measured concentration, n = number of samples, $\overline{Q}_i$ = average discharge during the period interval, Q_i = instantaneous discharge at sampling time, and $\overline{C}$ = mean solute concentrations from Eqs. (3)–(5).

- *Method 4* (M4) predicted solute concentrations with a regression model (concentration vs. discharge) (Johnson, 1979). Five regression models were tested (lineal, logarithmic, potential, exponential, and hyperbolic) and they were selected for each solute based on the best-fit Pearson correlation coefficient. The predicted solute concentrations were then derived in relation to discharges measured using the 5-min data.
- *Method 5* (M5) estimated solute concentrations by linearly interpolating between solute measurements (Schleppi et al., 2006), obtaining a 5-min concentration database from the 4-hourly data. The 5-min resolution estimations obtained from M4 and M5 were then multiplied by the corresponding discharge measurements and summed to obtain the total export rates (Eq. (7)).

$$Export = \Sigma\, C_{est} * Q_{inst} \tag{7}$$

where, C_{est} = estimated concentration and Q_{inst} = instantaneous discharge.

The input and export rates are shown in mEq km^{-2} yr^{-1} to give the same weight to all solutes regardless of the magnitude of their concentrations. Nevertheless, in order to compare the results with other studies, they are also presented in kg ha^{-1} yr^{-1} since mass fluxes are generally expressed in these units (Cerný et al., 1994).

2.6.3. Optimum sampling frequency for export calculation

The optimum sampling frequency for solute export was assessed creating subsets at lower frequencies: 8-hly (8 h), 12-hly (12*h*), daily (D), twice-weekly (TW), weekly (W), biweekly (B), and monthly (M). These sampling frequencies were selected as they are commonly used in water quality monitoring programs worldwide, and they were compared with the 4-hourly measurements. Export rates were then calculated for all frequencies and for each of the five methods previously described.

Additionally, we examined whether the sampling hour (i.e., time of day) influences the export rates. Values were removed from the database so that the sampling would always start at different hours: 02 h00, 06 h00, 10 h00, 14 h00, 18 h00, and 22 h00. This was done as a means of imitating a hypothetical fixed schedule where the sampling always takes place at the same hour.

2.7. Statistical analysis

The percent relative error (Eq. (8)) was used to estimate the difference between the export rates calculated with the five different methods as well as between the sampling frequencies. This metric was selected because merely evaluating absolute differences could be misleading. Relative errors express an unbiased unit-free metric that is useful when comparing and interpreting values in a purposeful context (Dawson et al., 2007). The export rates calculated with the interpolation method (M5) were taken as reference. A 10% difference or "error" from the best estimate (M5) was deemed as acceptable, as suggested by Swistock et al. (1997).

$$Error = \frac{Estimated\ export\ value - Reference\ export\ value}{Reference\ export\ value} * 100 \tag{8}$$

2.8. Input–export budgets and retention ratios

The solute budgets were calculated as the difference between input and export for each solute evaluated Eq. (9) (Cerný et al., 1994). Budgets were also calculated with the export rates from the filtered frequencies established earlier. A negative sign for the calculated budget reveals higher export than input, indicating geogenic and/or biologically active solutes produced and leached from within the catchment. A positive sign implies higher input than export, which is indicative of storage, adsorption and/

or sedimentation processes. A budget close to 0 points to steady state behavior.

$$Budget = Input - Export \quad (9)$$

Additionally, the retention ratio was calculated as a unit-free metric that is useful for comparison purposes (Eq. 10). In order to compare among solutes, we expressed this value as a percentage.

$$RR = \frac{Input - Export}{Input} * 100 \quad (10)$$

All analyses were carried out using R version 3.6.1 (R Core Team, 2019).

3. Results

3.1. Hydrometeorological and solute concentration dynamics

Fig. 2 shows the temporal dynamics for rainfall and discharge, along with selected solute (Si and DOC) concentrations over the study year 2018–2019. DOC and Si concentrations in rainfall water were almost constant throughout the year (sd = 1.58 mg L^{-1} and sd = 0.06 mg L^{-1}, respectively). Nonetheless, during the drier period (September–November), DOC increased (<10 mg L^{-1}), whereas Si decreased slightly (>0.1 mg L^{-1}).

The solute concentrations in stream water revealed more marked trends. DOC increased consistently with discharge, while Si decreased at higher discharges. These dynamics can also be seen in Appendix A, showing concentration-discharge relations and their *R* coefficients, as well as in Appendix B, which displays these concentration-discharge relations on a logarithmic scale. DOC and Si concentration-discharge correlations are reflected in the corresponding *R* coefficients (0.51 for DOC and − 0.49 for Si). The solutes Al, Cu, and TNb exhibited the same behavior as DOC, whereas Ca, K, Mg, Na, Rb, and Sr behaved similarly to Si. These similarities are supported by the Spearman correlation coefficients (r^2) between pairs of solutes (Appendix C).

The concentrations of nutrients and heavy metals did not manifest a clear relation with discharge or with other solutes, as reflected in low and insignificant *R* coefficients (mostly <0.2) (Appendices A, B, and C).

For a better visualization of the classified concentration-discharge relationships (Appendices D, E, F, and G), we selected three solutes that represent three behaviors with different dynamics during storm events (Fig. 3). DOC demonstrated a clear mobilization behavior for all events (Fig. 3 upper panel), in contrast to Si, which displayed an unambiguous dilution behavior (Fig. 3 middle panel). On the other hand, As exhibited chemostatic behavior (Fig. 3 lower panel), with a more marked trend during the events corresponding to the dry period. DOC was representative of the behavior of TNb, NH_4-N, Al, B, Cu, Fe, Zn, and Pb; while Si exemplified the behavior of Ca, K, Mg, Na, Rb, and Sr. Solutes such as PO_4, Ba, Cd, Cr, and V had different behaviors depending on the event period (wet or dry). The concentration-discharge relationships for all solutes can be seen in Appendices D, E, F, and G.

3.2. Rainfall solute inputs

Table 1 shows the rainfall input to solute budgets. DOC presented the largest annual input to the system with 4.17E + 08 mEq km^{-2} yr^{-1}. Nutrients such as TNb and NH_4-N also had high inputs, while PO_4 and NO_2-N presented the lowest nutrient supply. Among all cations, Si showed the greatest input with 1.72E + 07 mEq km^{-2} yr^{-1}. The base cations also exhibited high inputs as follows: Ca > Na > K > Mg. The remaining cations yielded minor rainfall inputs; the lowest being 1.77E + 03 mEq km^{-2} yr^{-1} for Rb. The input values were much lower for the heavy metals, with Cr showing the highest rate (5.52E + 04 mEq km^{-2} yr^{-1}) and Cd the lowest (1.69E + 03 mEq km^{-2} yr^{-1}). For comparison purposes, Appendix H shows the results from Table 1 in kg ha^{-1} yr^{-1} and the VWMC.

3.3. Solute export

3.3.1. Comparing different methods and performance

Evaluation of the performance of each method requires a reference or "benchmark" method that is assumed to provide the most accurate export

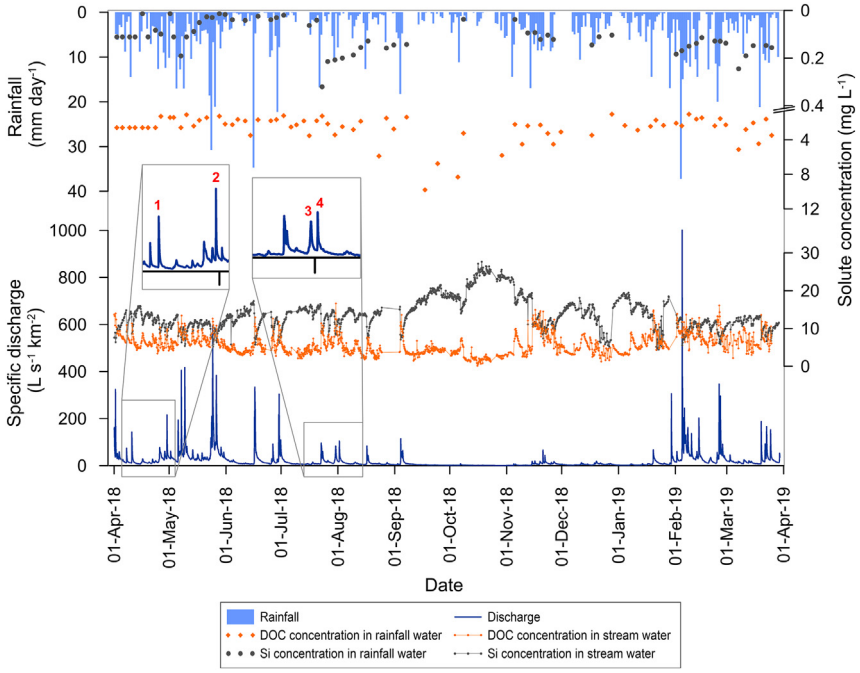

Fig. 2. Temporal variation (2018–2019) of the selected solutes, DOC (orange) and Si (grey). Rainfall volume is displayed on the scale at the top left of the figure and solute concentrations in rainfall water are displayed using the scale at the top right of the figure. Specific discharge is represented on the bottom left-hand scale of the figure and solute concentrations in stream water on the bottom right-hand scale of the figure. The zoom inlet panels with the numbers highlighted in red identify the four selected storm events used to analyze concentration-discharge relationships.

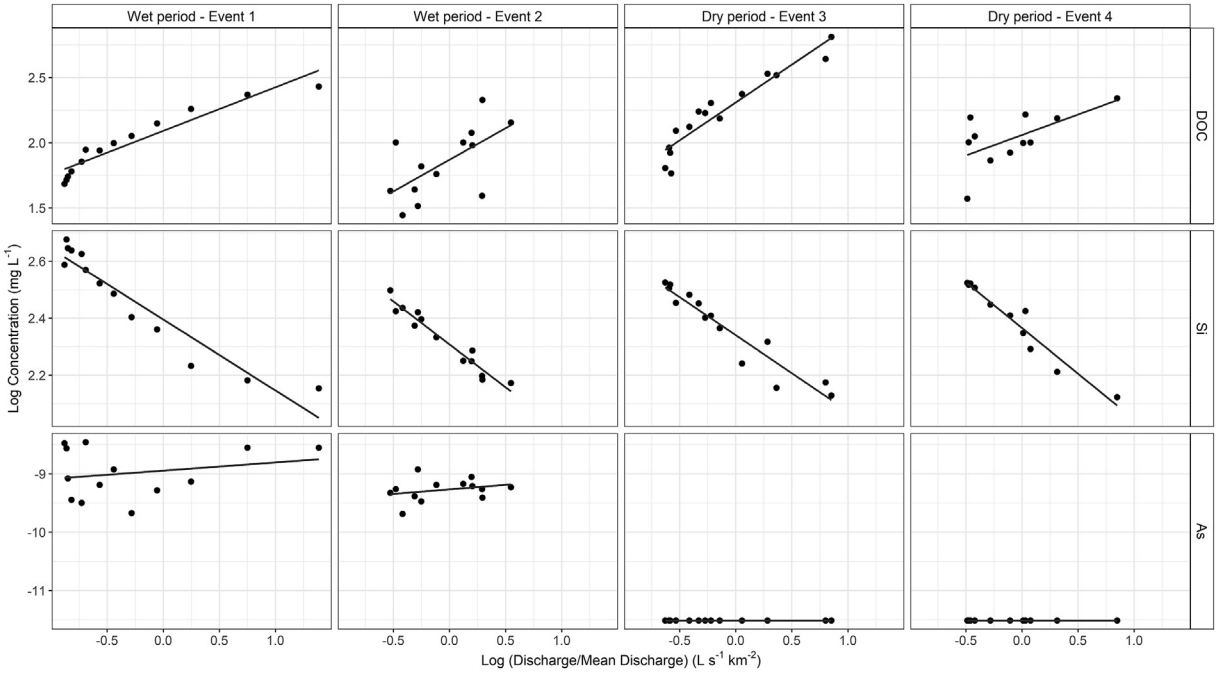

Fig. 3. Concentration-discharge relationship scatter plots on logarithmic axes indicating the three hydrochemical behaviors (under wet and dry conditions).

rate. The regression method (M4) is often used as reference, based on a flow-concentration curve. Here, even the 4-hourly data did not show strong correlations with discharge (Appendices A and B). The highest *R* coefficients were around 0.5 (for Si and DOC), with values as low as 0.01 for Cr. Therefore, the interpolation method (M5) was chosen as the reference method for comparisons across methods, as suggested by Aulenbach et al. (2016) (see Section 2.6.2. Export rates). Fig. 4 shows the export difference between M5 and the other methods analyzed at different sampling frequencies.

M1 reported significantly higher differences than the other methods, either under- or overestimating the export. Very few solutes reported differences below 10% (e.g., NH_4-N, PO_4, As, Cr). DOC, TNb, NO_3-N, PO_4, Al, Cu, Zn, and Cd were underestimated at all frequencies. NH_4-N, B, and Pb were also generally underestimated, although they had slight overestimations at certain frequencies. The highest underestimation with M1 was 35% for Cd with twice-weekly samples. By contrast, NO_2-N, Ca, Fe, K, Mg, Na, Rb, Si, Sr, As, Ba, and V presented overestimations at all frequencies, with a slight underestimation for As at a biweekly frequency. The highest overestimation with M1 was for Rb with a 50% difference at a monthly frequency.

M2 generally yielded export underestimations for all solutes. A few minor overestimations were found for some solutes (Fig. 4), with differences below 5% in most cases (e.g., Fe, Mg, Na, and V with twice-weekly samples or Mg, Na, Rb, and Zn with weekly samples). Solutes such as PO_4, Cr and Cd did not follow a pattern for different sampling frequencies, with Cd presenting both the highest under- and overestimation with M2 (21% and 40% difference, respectively).

Export calculated with M3 did not reveal a general pattern among solutes or sampling frequencies (Fig. 4). Solutes positively correlated with discharge were always overestimated (DOC, TNb, Al), the highest being 20% for daily TNb. This pattern was reversed for solutes negatively correlated with discharge (Ca, Mg, Na, Si), with differences up to 11% for biweekly Na. Cr was the only heavy metal with differences above 10% for M3. PO_4 reported the highest underestimation with a 38% difference using biweekly samples for M3. For certain solutes (e.g., B, Cu, Fe, K, Rb, Cd), this method appeared to be the one with the most similar export rates to those under M5, with all differences below 10%.

M4 yielded higher export differences than M2 and M3, as can be seen in Fig. 4. Ca, Fe, K, Mg, Na, Rb, Si, Sr, As, Ba, and V were underestimated at all sampling frequencies with M4. Rb presented the largest underestimations using this method, with the highest being 37% with twice-weekly sampling. DOC, Al, Cu, and Cd were always overestimated, with differences of up to 24% for Al at biweekly sampling. B presented the highest export overestimations with M4, with differences around 40%. Since the nutrients did not have a strong concentration-discharge relationship, they were randomly under- or overestimated, depending on the sampling frequency. NH_4-N and PO_4 presented higher differences (~ 25%) at lower sampling frequencies, starting at twice-weekly sampling frequencies.

Table 1
Rainfall inputs for the twenty-four solutes analyzed in mEq km^{-2} yr^{-1}.

Solute		Input (mEq km^{-2} yr^{-1})	Solute		Input (mEq km^{-2} yr^{-1})
Nutrients	DOC	4.167E+08	Cations	Al	4.177E+06
	TNb	1.701E+08		B	2.381E+05
	NH_4-N	4.750E+07		Ca	5.778E+06
	NO_2-N	1.696E+06		Cu	5.404E+04
	NO_3-N	1.759E+07		Fe	1.875E+06
	PO_4	1.998E+06		K	2.890E+06
Heavy metals	As	3.675E+03		Mg	2.177E+06
	Ba	2.142E+04		Na	4.376E+06
	Cd	1.686E+03		Rb	1.767E+03
	Cr	5.519E+04		Si	1.729E+07
	Pb	2.827E+03		Sr	2.009E+04
	V	1.054E+04		Zn	1.448E+06

3.3.2. Solute export rate estimates

Table 2 shows the export rates with M5 (the reference method) with the 4-hourly data. The highest export rates were Si with 2.95E+08 mEq km^{-2} yr^{-1}, followed by DOC with 2.69E+08 mEq km^{-2} yr^{-1} and TNb with 2.94E+07 mEq km^{-2} yr^{-1}. The base cations were exported according to the following order: Na > Ca > Mg > K, with 2.38E+07 mEq km^{-2} yr^{-1} for Na. Just as for the rainfall input, Rb presented the lowest cation export rate of 4.73E+03 mEq km^{-2} yr^{-1}. The nutrient NO_3-N showed an export rate of 2.63E+06 mEq km^{-2} yr^{-1} and PO_4 displayed a rate of 2.10E+05 mEq km^{-2} yr^{-1}. The heavy metals presented the lowest export rates of all solutes. The export of heavy metals ranged from 9.81E+04 mEq km^{-2} yr^{-1} for Ba to 8.36E+02 mEq km^{-2} yr^{-1} for As

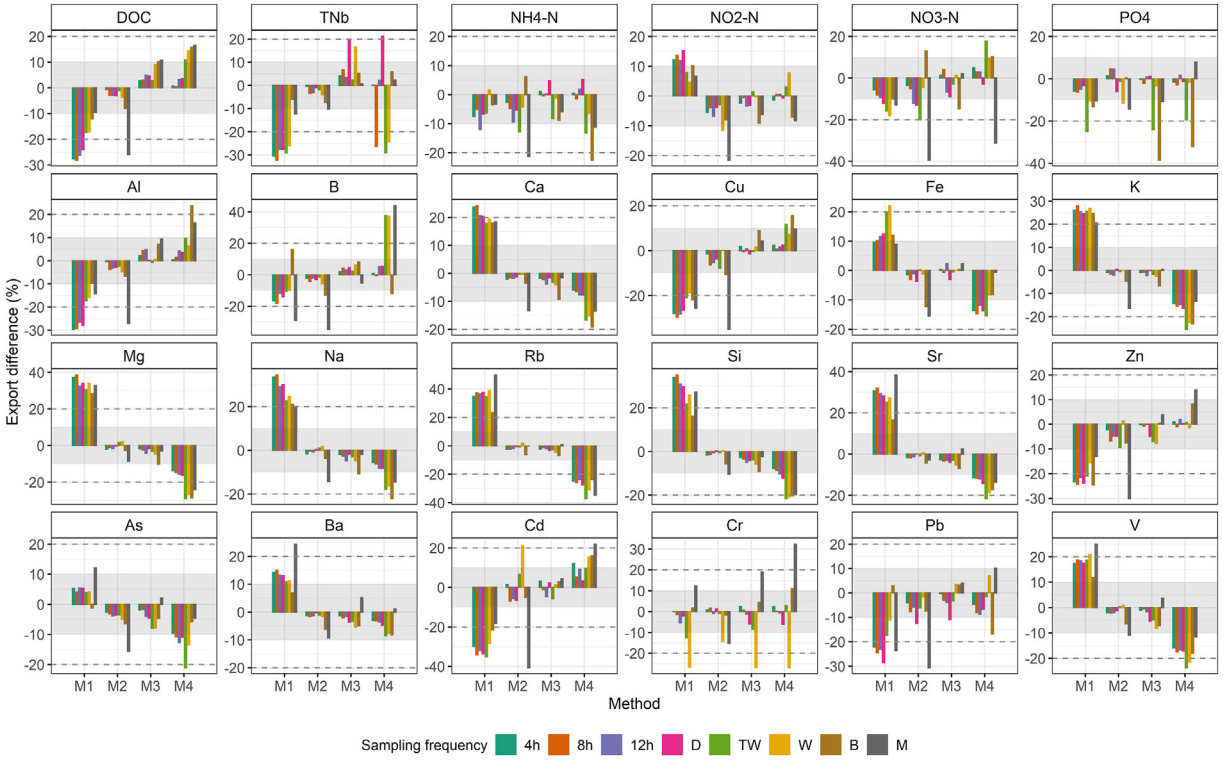

Fig. 4. Export differences between methods, using the interpolation method (M5) as reference. M1 = Sampling independently from the discharge; M2 = Measuring the average discharge for an interval between samples; M3 = Measuring instantaneous discharge at sampling time, and M4 = Regression model. 4 h = 4-hourly; 8 h = 8-hourly; 12 h = 12-hourly' D = Daily; TW = Twice-weekly; W = Weekly; B = Biweekly, and M = Monthly. The grey band highlights the ±10% export difference deemed as acceptable, and the dashed line represents a ± 20% difference.

(Table 2). The export rates at all analyzed sampling frequencies can be found in Appendix I (mEq km^{-2} yr^{-1}) and Appendix J (kg ha^{-1} yr^{-1}).

3.3.3. Optimum water quality sampling frequency

Fig. 5 shows 4-hourly solute export compared to all other frequencies calculated using M5 to evaluate the effect of the sampling frequency on export rates. The 8-hourly, 12-hourly and daily export showed differences below 10% for any sampling hour with few exceptions (notably daily NO_3-N). Higher than daily sampling frequencies resulted in increasing differences and in a stronger influence of the sampling hour on export estimates.

The nutrients presented random under- and overestimations depending on the sampling hour (Fig. 5) with twice-weekly sampling. For instance, NO_3-N was underestimated at 22 h00, but at 10 h00 it was overestimated, with differences of around 20%. PO_4 presented the largest nutrient overestimation at the twice-weekly sampling frequency, with a 42% difference (at 10 h00). The cations showed steady results as the resolution was lowered, with an average difference increase of 4%. Cr presented the largest heavy metal overestimation with a 35% difference (at 10 h00).

At a weekly and biweekly sampling frequencies, the differences increased further for almost all solutes, generally yielding underestimations at any sampling hour (Fig. 5). Monthly sampling resulted in large and fluctuating differences (Fig. 5), such as a 30% underestimation at 06 h00 for DOC.

Table 2
4-hourly export rates calculated using the interpolation method (M5) for the twenty-four solutes in mEq km^{-2} yr^{-1}.

	Solute	4-hourly Export (mEq km^{-2} yr^{-1})	Solute		4-hourly Export (mEq km^{-2} yr^{-1})
Nutrients	DOC	2.686E+08	Cations	Al	2.184E+06
	TNb	2.940E+07		B	9.083E+04
	NH_4-N	1.612E+06		Ca	1.709E+07
	NO_2-N	3.920E+05		Cu	4.665E+04
	NO_3-N	2.630E+06		Fe	1.603E+06
	PO_4	2.100E+05		K	4.368E+06
Heavy Metals	As	8.358E+02		Mg	7.593E+06
	Ba	9.809E+04		Na	2.379E+07
	Cd	1.248E+03		Rb	4.725E+03
	Cr	7.143E+03		Si	2.953E+08
	Pb	1.756E+03		Sr	2.673E+05
	V	2.932E+03		Zn	1.648E+05

3.4. Total solute budgets and retention ratios

The total solute budgets subtract the annual export from rainfall input rates. A positive budget represents an accumulation of a certain solute in the catchment, whereas a negative value implies that the given solute is being removed (Cerný et al., 1994). Fig. 6 shows the retention ratio (in percentage) with the 4-hourly export results. Most solutes exhibited positive budgets indicating greater inputs than export, as can be seen from Fig. 6. DOC and TNb had the highest positive budgets with 1.48E+08 mEq km^{-2} yr^{-1} (64%) and 1.41E+08 mEq km^{-2} yr^{-1} (17%), respectively. All nutrients were accumulated in the system (positive budgets), ranging from 4.59E+07 mEq km^{-2} yr^{-1} (3%) for NH_4-N to 1.30E+06 mEq km^{-2} yr^{-1} (23%) for NO_2-N. Heavy metals (except for Ba) were also accumulated in the catchment, with the highest and lowest budgets ranging from 4.81E+04 mEq km^{-2} yr^{-1} (13%) for Cr to 4.38E+02 mEq km^{-2} yr^{-1} (74%) for Cd. The only cations that presented positive budgets were Al, Zn, Fe, B, and Cu, ranging from 1.99 E+06 mEq km^{-2} yr^{-1} (52%) for Al to 7.39E+03 mEq km^{-2} yr^{-1} (86%) for Cu.

By contrast, the base cations Si, Na, Ca, Mg, and K presented negative budgets. These budgets ranged from −2.78E+08 mEq km^{-2} yr^{-1} (1707%) for Si to −1.48E+06 mEq km^{-2} yr^{-1} (151%) for K. Both, positive and negative budgets were constant for all tested sampling frequencies (Appendices K and L), regardless of the reported export under- or overestimations.

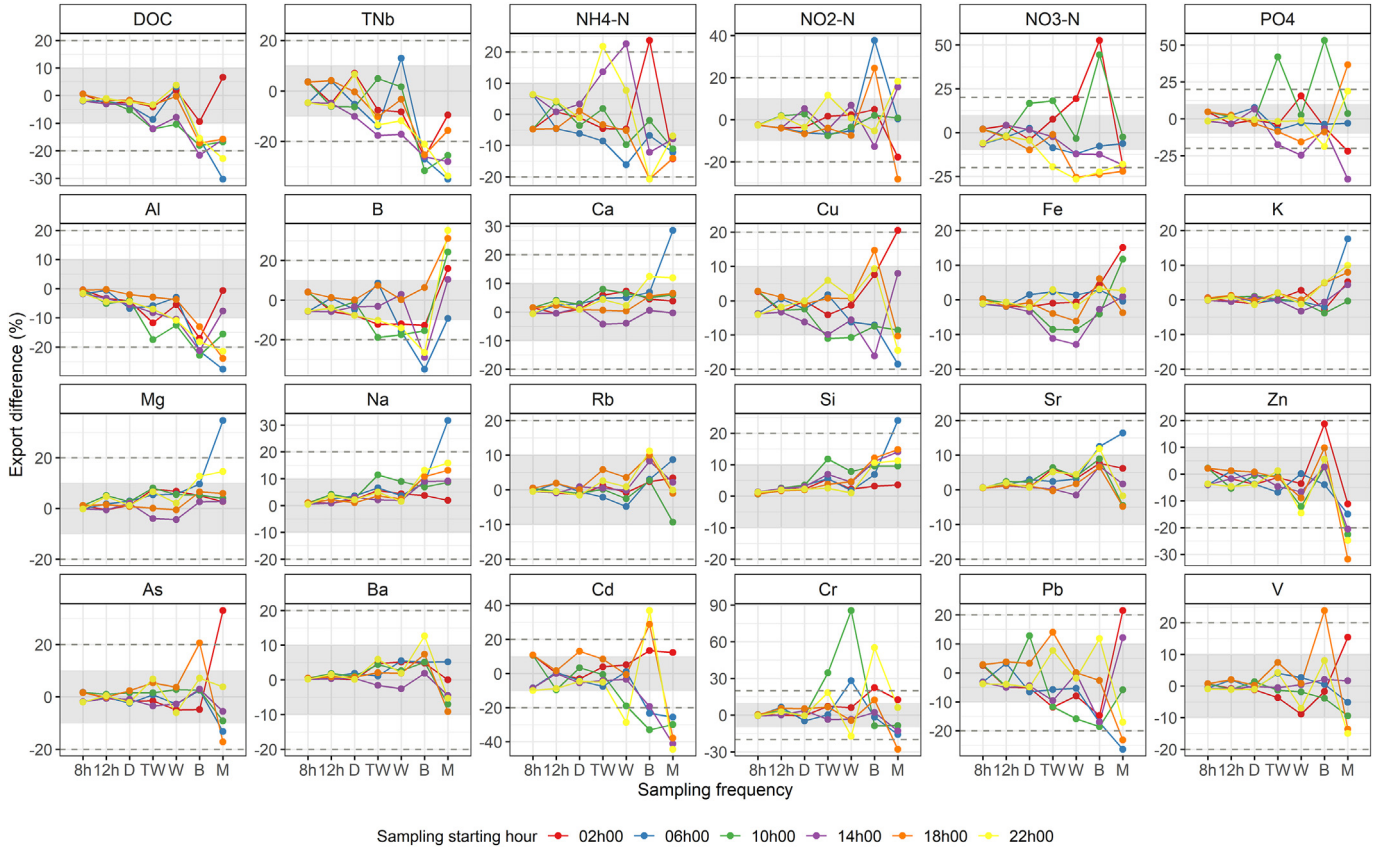

Fig. 5. Export differences between different sampling frequencies and the the 4-hourly benchmark data using M5. 8 h = 8-hour; 12 h = 12-hour; D = Daily; TW = Twice-weekly; W = Weekly; B = Biweekly, and M = Monthly. The grey band highlights the ±10% export difference deemed as acceptable, while the dashed line represents a ± 20% difference.

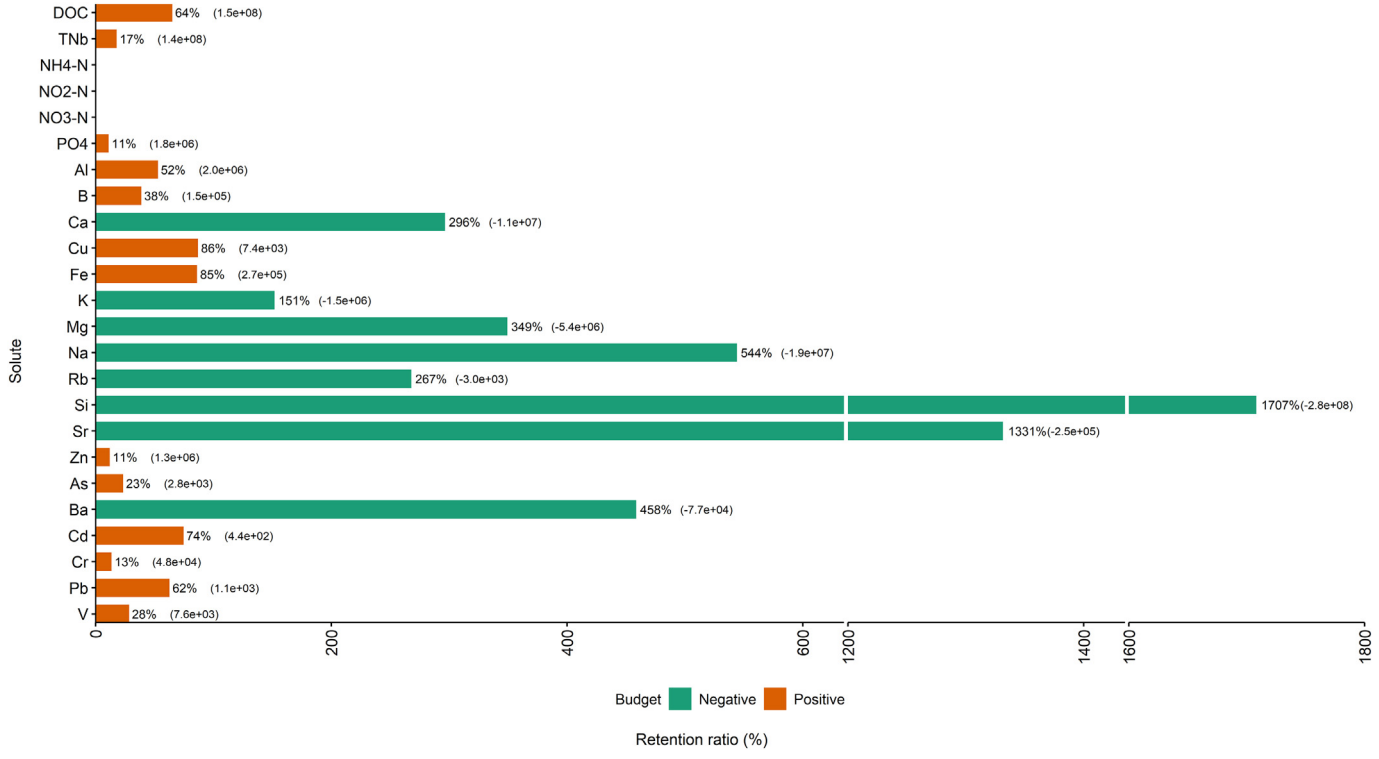

Fig. 6. Solute retention ratios. Negative budgets are presented in green and positive budgets are presented in orange. The numbers in parenthesis represent the budget value in mEq km^{-2} calculated with export rates for the 4-hourly sampling frequency using the interpolation method (M5).

4. Discussion

4.1. Chemical rainfall input composition in the Andean páramo

Our study revealed that rainwater had high concentrations of DOC and TNb. The VWMC (Appendix H) (1.91 mg L^{-1} for DOC and 0.91 mg L^{-1} for TNb) were comparable to those found in a tropical montane forest in southern Ecuador with an average DOC concentration of 4.3 mg L^{-1} and 0.42 mg L^{-1} for TNb (Goller et al., 2006). Similarly, NH_4-N (3.32 kg ha^{-1} yr^{-1}) and NO_3-N (1.23 kg ha^{-1} yr^{-1}) inputs were comparable to the montane forest: 2.6 kg ha^{-1} yr^{-1} for NH_4-N and 3 kg ha^{-1} yr^{-1} for NO_3-N (Wilcke et al., 2001). The high DOC and nutrient input could be explained by precipitation frequently originating from the western Andean slopes of the Amazon (Buytaert et al., 2006a, 2006b; Esquivel-Hernández et al., 2019; Vuille et al., 2000). Tropical forests are characterized by high concentrations of C, N, and P compounds (Möller et al., 2005; Shanley et al., 2011) in rainfall, throughfall, and litter leachate, which may explain the high inputs of these solutes to the ecosystem.

The base cations presented lower input rates in the catchment area than in montane forests, with values around 1 kg ha^{-1} yr^{-1} for Ca, Na, and K (Appendix H); while in the forest, average rates of 5.6 kg ha^{-1} yr^{-1} of Ca, 4.3 kg ha^{-1} yr^{-1} of Na, and 8 kg ha^{-1} yr^{-1} of K (Bücker et al., 2011), and 3.9 kg ha^{-1} yr^{-1} of Ca, 19 kg ha^{-1} yr^{-1} of Na, and 3.7 kg ha^{-1} yr^{-1} of K (Wilcke et al., 2001) have been reported. The slightly higher cation input rates in the montane forest may be attributed to solute recycling leached from leaves (Wilcke et al., 2001). Additionally, there has been an increase in the concentration of cations in the last decade due to fires in the Amazon forest (Wilcke et al., 2020). To the best of our knowledge, no literature is available to compare with our calculated input rates for the remaining cations (B, Cu, Rb, Si, and Sr) and heavy metals.

4.2. Export calculation methods, sampling frequency and hour

The use of M5 as the reference method stands in contrast to previous studies that have found the regression method to work best (Johnson, 1979; Swistock et al., 1997). However, these studies reported strong concentration-discharge relationships with R coefficients between 0.68 and 0.91 for Al (Swistock et al., 1997) compared to $R = 0.48$ found here. Likewise, Schleppi et al. (2006) found determination coefficients (r^2) greater than 0.8 for Ca and Mg. Here, R coefficients below 0 were found for both solutes. The export method should be selected based on flow variability, sampling resolution and design, and the strength of the concentration-discharge relations (Aulenbach et al., 2016; Shih et al., 2016). In this sense, the interpolation method is a reasonable approach for solutes with weak or non-existent concentration-discharge relations.

M1 consistently reported the highest differences among all methods compared. Because this method does not consider discharge, base-flows are overrepresented in the mean solute concentrations, since the same weight is assigned to all concentration values. The cations that are negatively correlated with discharge presented significant overestimations under M1 (Fig. 4). These findings were also reported by Schleppi et al. (2006) for a small mountain stream in Switzerland. This effect is reversed when solutes are positively correlated with discharge (Walling and Webb, 1985), since most of the export occurs during high flows. Such is the case for DOC, TNb, Al, Cu, Zn, and Cd, which consistently yielded underestimated export rates using M1.

M2 showed lower differences than M1 and M4, but export rates were always underestimated. These findings may be explained by the fact that when the average discharge is considered, particularly in low-frequency sampling schemes, storm-flow conditions are under-represented, thereby resulting in lower export rates (Aulenbach et al., 2016; Dann et al., 1986; Hopkins et al., 2017; Johnson, 1979).

M3 had differences mainly below 10% for most solutes (DOC, cations, and most heavy metals). The FWMC method is commonly used in export studies since the concentrations are weighted by the instantaneous discharge and small changes are more sensitive with high-frequency data. The M3 4-hourly export rates were similar to the 5-min interpolated data (M5).

M4 overestimated the export for solutes positively correlated with discharge and underestimated export for negatively correlated solutes (contrary to M1). Regression-based methods generally emphasize high flows with higher contributions to the total solute export (Dann et al., 1986). Additionally, at lower sampling frequencies, the 4-hourly best-fit regression function and parameters no longer applied, indicating potentially misleading models. As a result, M4 exhibited high export differences, particularly at lower sampling frequencies (Fig. 5). This finding further supports the use of M5 as the reference model.

Overall, Si (20.73 kg ha^{-1} yr^{-1}), Na (5.47 kg ha^{-1} yr^{-1}), Ca (3.43 kg ha^{-1} yr^{-1}), Mg (0.93 kg ha^{-1} yr^{-1}), and K (1.71 kg ha^{-1} yr^{-1}) were the cations with the highest export (Appendix J). The findings are comparable to a tropical montane forest in southern Ecuador with 11–14 kg ha^{-1} yr^{-1} for Na, 6–8 kg ha^{-1} yr^{-1} for Ca, 4–5 kg ha^{-1} yr^{-1} for Mg, and 7–8 kg ha^{-1} yr^{-1} for K (Bücker et al., 2011). The relatively larger export rates in the forested catchment may be attributed to tree canopies effectively trapping dry deposition from the atmosphere (Finér et al., 2004). Export of these cations is generally associated to weathering of the parental material (McDowell et al., 1995; Musolff et al., 2015; Reynolds et al., 1997), and weathering rates can be particularly high in tropical humid ecosystems as they are amplified by large amounts of CO_2 in the surrounding soil atmosphere (Bhatt and McDowell, 2007; McDowell et al., 1995; McDowell and Asbury, 1994). Additionally, small volcanic watersheds tend to have high cation stream concentrations (Wymore et al., 2017). No other studies of tropical environments could be found to compare to the calculated export of Rb or Sr in the catchment area, although sources of these solutes are primarily attributed to weathering of plagioclase (Turner et al., 2010). This is corroborated by a study in the ZEO, where Correa et al. (2019) found the same sources and concentration-discharge relations for these solutes as for the base cations (Fig. 4). Large DOC export (16.13 kg ha^{-1} yr^{-1}) may be due to the high amounts of organic carbon in the soils and that runoff in this ecosystem is mainly generated from the wetlands/Histosols (Lazo et al., 2019; Pesántez et al., 2018). For a tropical rainforest catchment in Costa Rica, Sánchez-Murillo et al. (2019) found significantly lower DOC values, with an average annual rate of 6.70E-07 kg ha^{-1}. Aitkenhead-Peterson et al. (2007), found export rates ranging from 1.7E+05 kg ha^{-1} yr^{-1} to 1.05E+06 kg ha^{-1} yr^{-1} in 56 streams in Scotland with similar soil conditions (peatlands) but a temperate climate (Aitkenhead et al., 1999). See also Sánchez-Murillo et al. (2019) for a comparison of literature on DOC export in tropical and global streams.

Solutes with a similar concentration-discharge relationship to DOC are assumed to be exported in parallel. For instance, TNb is exported during high flows by leaching (Ritson et al., 2019). Likewise, Correa et al. (2017) demonstrated that Al and Fe sources in the study site are mainly shallow soil horizons. Both solutes contribute to the accumulation of carbon in soils when organometallic complexes are formed due to volcanic ash breakdown (Buytaert et al., 2006a, 2006b, 2006c). This may imply that these solutes are also exported along with DOC as described by Knorr (2013) and Kortelainen et al. (2006). The Al export rate (1.97E-01 kg ha^{-1} yr^{-1}) was similar to that found by Boy et al. (2008) in the tropical montane forest, where the average export was 3.03E-01 kg ha^{-1} yr^{-1}, while Fe export (4.48E-01 kg ha^{-1} yr^{-1}) was much lower than that which Kortelainen et al. (2006) reported as an average for Finnish catchments (2.8E+04 kg ha^{-1} yr^{-1}). Cu and Zn presented higher concentrations at higher discharge levels (Fig. 3, Appendices A, D, E, F, and G). Previous studies in different ecosystems have reported similar patterns, such as Wilcke et al. (2001) for tropical montane forests or Xue et al. (2000) for a small agricultural catchment in Switzerland.

The nutrients NH_4-N (1.13E-01 kg ha^{-1} yr^{-1}) and NO_3-N (1.84E-01 kg ha^{-1} yr^{-1}), displayed export rates that were somewhat similar to those found in other tropical catchments. Boy et al. (2008) found average export rates of 1.4 kg ha^{-1} yr^{-1} for NH_4-N and 1.06 kg ha^{-1} yr^{-1} for NO_3-N in a montane forest, and Germer et al. (2009), found 1.95 kg ha^{-1} yr^{-1} for

NH_4-N and 0.3 kg ha^{-1} yr^{-1} for NO_3-N in an undisturbed amazon catchment in Brasil. The slightly higher results are coherent since both are forested catchments and nutrient concentrations tend to be higher in such catchments due to increased biotic demand (Goodale et al., 2000). Furthermore, Huang et al. (2012) found average NO_3-N yields of 58,500 kg km^{-2} yr^{-1} in three relatively pristine subtropical forested catchments in Taiwan. This value may point to increased export rates caused by the use of fertilizers (Huang et al., 2012).

Heavy metals concentrations in undisturbed catchments can also be associated with physical weathering. In the ZEO, Correa et al. (2019) found the highest concentrations of Ba and V in spring water, suggesting deeper geogenic sources. For an agricultural catchment in France, the export rates were significantly larger, with 100 kg ha^{-1} yr^{-1} for As, 3 kg ha^{-1} yr^{-1} for Cd, 410 kg ha^{-1} yr^{-1} for Cr, and 110 kg ha^{-1} yr^{-1} for Pb, which is attributed to the use of pesticides (Roussiez et al., 2013). Similarly, on a former mining watershed in France, the export rates were 2119 kg of As, 24.5 kg of Cd, and 2360 kg of Pb for just a single 24-h event sampled every hour (Resongles et al., 2015).

The concentration-discharge relations demonstrated that DOC, TNb, Al, Cu, Fe, and Zn concentrations increase with discharge. As stated before, these solutes are exported from shallow horizons during storm events, which indicates a mobilization behavior in line with Moatar et al. (2017) and Wymore et al. (2017). By contrast, base cations such as Si, Ca, K, Mg, and Na weathering sources were characterized by a decrease in solute concentrations during storm events, representing a dilution behavior. Similar findings were reported in other tropical volcanic catchments in Puerto Rico (Stallard and Murphy, 2014; Wymore et al., 2017). The nutrients and heavy metals showed random variations in their concentrations, displaying different behaviors depending on the storm event analyzed (Appendices D, E, F, and G).

Due to the availability of 4-hourly high-frequency data, various sampling schemes could be tested to determine the minimum acceptable monitoring frequency without compromising the export results. As expected, sampling frequencies beyond daily yielded the highest export differences with the reference method (beyond 10%) in our study site (Fig. 5). They would also imply a cost reduction of around 80% in our study. This cost estimate includes sample collection and analysis, transportation, and human resources.

These results reflect those of Tang et al. (2008), who reported N and P underestimations of 30% with weekly samples in a Chinese subtropical catchment. Additionally, these results further support the idea that monthly to weekly samples are not reliable to draw conclusions about a catchment's hydrochemical behavior (Kirchner et al., 2004).

Our study also found that for DOC and most cations no relevant effect of the sampling hour was identified, with differences mainly below 10%. These results would imply that sampling could be done during any time of the day, regardless of the sampling frequency. However, this is not the case for nutrients and heavy metals. The export rates were randomly under- or overestimated depending on the sampling hour, particularly at lower frequencies. These findings may be related to specific ecosystem hydrometeorological and biogeochemical processes. In the ZEO, Correa et al. (2017), Lazo et al. (2019), and Mosquera et al. (2015) have highlighted the importance of wetland contributions to runoff generation. Hence, a possible explanation might be that rainfall in the ZEO is predominant during the afternoon hours (Carrillo-Rojas et al., 2019; Padrón et al., 2015), which would produce soil water recharge at night and consequently an export from shallow horizons. As for heavy metals, Walling and Webb (1985) indicate that the degree of under- or overestimation will depend on the concentration variability of each solute. This statement becomes true for heavy metals because of their particularly low concentrations, where a small variation can be significant.

4.3. Negative and positive total solute budgets in a páramo ecosystem

The majority of the solutes presented positive budgets considering that rainfall inputs were not particularly high nor the export rates particularly low. This would imply that the catchment is accumulating solutes. These results may even be understated since only rainfall input was considered, and fog and dew are presumed to be an important input in cloudy humid ecosystems (Bendix et al., 2008; Buytaert et al., 2006a, 2006b, 2006c; Schmitt et al., 2018). These additional solute inputs are yet to be studied.

DOC and TNb exhibited the highest net gains among all solutes analyzed. These findings may suggest that rainfall is an important source of carbon to the ecosystem, contributing to the large carbon storage in soils and therefore to carbon in stream water. However, Carrillo-Rojas et al. (2019) demonstrated that the ZEO acts as a source of atmospheric carbon.

Si and the base cations (Na, Ca, Mg, and K) presented the highest export rates during the study period. These findings imply that the catchment is releasing Si and base cations to stream water. These solutes are associated with geological weathering and are released from the same sources (Correa et al., 2017). Some researchers have studied different scenarios in which rock weathering may be altered. For instance, in future climate-change scenarios where temperature, precipitation, and atmospheric CO_2 levels are expected to increase, weathering is assumed to be dramatically enhanced (Hung et al., 2020; Lindberg and Turner, 1988; Qafoku, 2015). In fact, Gislason et al. (2009) demonstrated that weathering rates have already been increasing over the past four decades as a consequence of global warming. Moreover, Kaushal et al. (2017), suggested that urbanization can also increase the export of solute concentration of cations from headwater catchments to downstream receiving bodies. These findings could pose challenges for water purification plants, irrigation systems, water distribution, and even long-term health risks.

5. Conclusions

This study aimed to quantify solute fluxes in a páramo ecosystem testing different commonly used export methods and to establish an optimum sampling frequency to be used in water quality monitoring programs.

The solute fluxes revealed that this ecosystem has high concentrations of DOC, TNb, Si, and base cations. They also showed that streamwater from the páramo naturally contains heavy metals due to the volcanic origin of the soils. These values are likely to rise due to enhanced weathering rates caused by climate change-induced increased atmospheric emissions. Concentration-discharge relationships revealed clear solute dynamics of discharge, with DOC, TNb, Al, Fe, and Cu representing mobilization behaviors, and Ca, K, Mg, Na, and Si representing dilution behaviors. These findings can be used as a baseline for possible water quality alterations in páramo headwaters in the future.

The selection of the most suitable export method for each ecosystem should be based on several factors, including sampling frequency, sampling representativeness of the entire range of flows, the strength of the concentration-discharge relationships, and discharge variability. In this páramo ecosystem, the interpolation method was found to be the most appropriate for 4-hourly data.

A minimum of daily stream samples is recommended in order to estimate export rates accurately ($\leq$ 10% difference) and avoid severe underestimations at lower sampling frequencies. However, the sampling hour may be an important issue to consider if nutrients or heavy metals will be analyzed. These results will help optimize and/or reduce monitoring resources and establish proper long-term sampling programs at low cost and maintenance, according to the research needs. Future research should consider fog and dew water inputs to solute budgets.

CRediT authorship contribution statement

Viviana Arízaga-Idrovo: Conceptualization, Methodology, Software, Formal analysis, Investigation, Data Curation, Writing Original Draft, Visualization.

Juan Pesántez: Conceptualization, Methodology, Data curation, Writing - Review & Editing, Supervision.

Christian Birkel: Validation, Writing - Review & Editing, Supervision.

Pablo Peña: Software, Resources.

Enma Mora: Resources, Formal analysis.

Patricio Crespo: Conceptualization, Validation, Writing - Review & Editing, Supervision, Project administration, Funding acquisition.

Funding

This research was funded by the Ecuadorian Secretary of Higher Education, Science, Technology and Innovation (SENESCYT) in the framework of the project "Desarrollo de Indicadores Hidrológicos Funcionales para la Evaluación del Impacto del Cambio Global en Ecosistemas Andinos", and by the IAEA research contract 22906 in the framework of the project "Evaluation of Non-Stationary Hydrological Conditions in the Andean Páramo".

Declaration of competing interest

The authors declare the following financial interests/personal relationships which may be considered as potential competing interests:

Patricio Crespo reports financial support was provided by International Atomic Energy Agency (IAEA). Patricio Crespo reports financial support was provided by Ecuadorian Secretary of Higher Education, Science, Technology and Innovation (SENESCYT).

Acknowledgments

This manuscript is an outcome of the University of Cuenca's Masters Program in Hydrology, with a mention in Ecohydrology. We are grateful to the Comuna Chumblín-Sombrederas of San Fernando-Azuay for the access we were granted to its community land reserve. We would also like to thank the INV Metals S.A. team for their assistance in the logistics during field work at the Zhurucay Ecohydrological Observatory. We also extend our thanks to the researchers and staff of the Departamento de Recursos Hídricos y Ciencias Ambientales, iDRHiCA, who contributed to sample collection and filtering. Special thanks are due to McDonald Benjamin and the two anonymous reviewers for their constructive criticism to improve the quality of our paper.

Appendix A. Supplementary data

Supplementary data to this article can be found online at https://doi.org/10.1016/j.scitotenv.2022.155560.

References

Aitkenhead-Peterson, J.A., Smart, R.P., Aitkenhead, M.J., Cresser, M.S., McDowell, W.H., 2007. Spatial and temporal variation of dissolved organic carbon export from gauged and ungauged watersheds of Dee Valley, Scotland: effect of land cover and C:N. Water Resour. Res. 43 (5), 1–11. https://doi.org/10.1029/2006WR004999.

Aitkenhead, J.A., Hope, D., Billett, M.F., 1999. The relationship between dissolved organic carbon in stream water and soil organic carbon pools at different spatial scales. Hydrol. Process. 1302 (July 1998), 1289–1302.

Aulenbach, B.T., Burns, D.A., Shanley, J.B., Yanai, R.D., Bae, K., Wild, A.D., Yang, Y., Yi, D., 2016. Approaches to stream solute load estimation for solutes with varying dynamics from five diverse small watersheds. Ecosphere 7 (6), 1–22. https://doi.org/10.1002/ecs2.1298.

Bendix, J., Rollenbeck, R., Richter, M., Fabian, P., Emck, P., 2008. 8: climate. Gradients in a Tropical Mountain Ecosystem of Ecuador. 2007, pp. 63–73.

Bhatt, M.P., McDowell, W.H., 2007. Controls on major solutes within the drainage network of a rapidly weathering tropical watershed. Water Resour. Res. 43 (11), 1–9. https://doi.org/10.1029/2007WR005915.

Borbor-Cordova, M.J., Boyer, E.W., McDowell, W.H., Hall, C.A.S., 2006. Nitrogen and phosphorus budgets for a tropical watershed impacted by agricultural land use: Guayas, Ecuador Nitrogen and phosphorus budgets for a tropical watershed impacted by agricultural land use: GuayasEcuador. Biochemistry 79 (July), 135–161. https://doi.org/10.1007/s10533-006-9009-7.

Boy, J., Valarezo, C., Wilcke, W., 2008. Water flow paths in soil control element exports in an Andean tropical montane forest. Eur. J. Soil Sci. 59 (6), 1209–1227. https://doi.org/10.1111/j.1365-2389.2008.01063.x.

Bücker, A., Crespo, P., Frede, H.G., Breuer, L., 2011. Solute behaviour and export rates in neotropical montane catchments under different land-uses. J. Trop. Ecol. 27 (3), 305–317. https://doi.org/10.1017/S0266467410000787.

Buytaert, W., Célleri, R., De Bièvre, B., Cisneros, F., Wyseure, G., Deckers, J., Hofstede, R., 2006. Human impact on the hydrology of the Andean páramos. Earth Sci. Rev. 79 (1–2), 53–72. https://doi.org/10.1016/j.earscirev.2006.06.002.

Buytaert, W., Celleri, R., Willems, P., Bièvre, B.De, Wyseure, G., 2006. Spatial and temporal rainfall variability in mountainous areas: a case study from the south Ecuadorian Andes. J. Hydrol. 329 (3–4), 413–421. https://doi.org/10.1016/j.jhydrol.2006.02.031.

Buytaert, W., De Bièvre, B., 2012. Water for cities: the impact of climate change and demographic growth in the tropical Andes. Water Resour. Res. 48 (8), 1–13. https://doi.org/10.1029/2011WR011755.

Buytaert, W., Deckers, J., Wyseure, G., 2006. Description and classification of nonallophanic Andosols in south Ecuadorian alpine grasslands (páramo). Geomorphology 73 (3–4), 207–221. https://doi.org/10.1016/j.geomorph.2005.06.012.

Buytaert, W., Iñiguez, V., De Bièvre, B., 2007. The effects of afforestation and cultivation on water yield in the Andean páramo. For. Ecol. Manag. 251 (1–2), 22–30. https://doi.org/10.1016/j.foreco.2007.06.035.

Carrillo-Rojas, G., Silva, B., Rollenbeck, R., Célleri, R., Bendix, J., 2019. The breathing of the Andean highlands: Net ecosystem exchange and evapotranspiration over the Páramo of southern Ecuador. Agric. For. Meteorol. 265 (March 2018), 30–47. https://doi.org/10.1016/j.agrformet.2018.11.006.

Cerný, J., Billett, M.F., Cresser, M.S., 1994. Element budgets. In: Moldan, B., Cerný, J. (Eds.), Biogeochemistry of Small Catchmentsvol. 51. John Wiley & Sons,Ltd, pp. 189–205. https://doi.org/10.1016/S0925-8574(00)00143-9.

Coltorti, M., Ollier, C.D., 2000. Geomorphic and tectonic evolution of the Ecuadorian Andes. Geomorphology 32 (1–2), 1–19. https://doi.org/10.1016/S0169-555X(99)00036-7.

Córdova, M., Carrillo-Rojas, G., Crespo, P., Wilcox, B.P., Célleri, R., 2015. Evaluation of the Penman-Monteith (FAO 56 PM) method for calculating reference evapotranspiration using limited data. Mt. Res. Dev. 35 (3), 230–239. https://doi.org/10.1659/MRD-JOURNAL-D-14-0024.1.

Correa, A., Breuer, L., Crespo, P., Célleri, R., Feyen, J., Birkel, C., Silva, C., Windhorst, D., 2019. Spatially distributed hydro-chemical data with temporally high-resolution is needed to adequately assess the hydrological functioning of headwater catchments. Sci. Total Environ. 651, 1613–1626. https://doi.org/10.1016/j.scitotenv.2018.09.189.

Correa, A., Windhorst, D., Tetzlaff, D., Crespo, P., Célleri, R., Feyen, J., Breuer, L., 2017. Temporal dynamics in dominant runoff sources and flow paths in the Andean Páramo. Water Resour. Res. 5 (3), 2. https://doi.org/10.1111/j.1752-1688.1969.tb04897.x.

Crespo, P., Feyen, J., Buytaert, W., Bücker, A., Breuer, L., Frede, H.G., Ramírez, M., 2011. Identifying controls of the rainfall-runoff response of small catchments in the tropical Andes (Ecuador). J. Hydrol. 407 (1–4), 164–174. https://doi.org/10.1016/j.jhydrol.2011.07.021.

Dann, M.S., Lynch, J.A., Corbett, E.S., 1986. Comparison of methods for estimating sulfate export from a forested watershed. J. Environ. Qual. 15 (2), 2–7. https://doi.org/10.2134/jeq1986.00472425001500020011x.

Dawson, C.W., Abrahart, R.J., See, L.M., 2007. HydroTest: a web-based toolbox of evaluation metrics for the standardised assessment of hydrological forecasts. Environ. Model. Softw. 22 (7), 1034–1052. https://doi.org/10.1016/j.envsoft.2006.06.008.

Esquivel-Hernández, G., Mosquera, G.M., Sánchez-Murillo, R., Quesada-Román, A., Birkel, C., Crespo, P., Célleri, R., Windhorst, D., Breuer, L., Boll, J., 2019. Moisture transport and seasonal variations in the stable isotopic composition of rainfall in Central American and Andean Páramo during El Niño conditions (2015–2016). Hydrol. Process. 33 (13), 1802–1817. https://doi.org/10.1002/hyp.13438.

Finér, L., Kortelainen, P., Mattsson, T., Ahtiainen, M., Kubin, E., Sallantaus, T., 2004. Sulphate and base cation concentrations and export in streams from unmanaged forested catchments in Finland. For. Ecol. Manag. 195 (1–2), 115–128. https://doi.org/10.1016/j.foreco.2004.02.040.

Germer, S., Neill, C., Vetter, T., Chaves, J., Krusche, A.V., Helmut, E., 2009. Implications of long-term land-use change for the hydrology and solute budgets of small catchments in Amazonia. J. Hydrol. 364 (3–4), 349–363. https://doi.org/10.1016/j.jhydrol.2008.11.013.

Gislason, S.R., Oelkers, E.H., Eiriksdottir, E.S., Kardjilov, M.I., Gisladottir, G., Sigfusson, B., Snorrason, A., Elefsen, S., Hardardottir, J., Torssander, P., Oskarsson, N., 2009. Direct evidence of the feedback between climate and weathering. Earth Planet. Sci. Lett. 277 (1–2), 213–222. https://doi.org/10.1016/j.epsl.2008.10.018.

Godsey, S.E., Kirchner, J.W., Clow, D.W., 2009. Concentration-discharge relationships reflect chemostatic characteristics of US catchments. Hydrol. Process. 23 (13), 1844–1864. https://doi.org/10.1002/hyp.7315.

Goller, R., Wilcke, W., Fleischbein, K., Valarezo, C., Zech, W., 2006. Dissolved nitrogen, phosphorus, and sulfur forms in the ecosystem fluxes of a montane forest in Ecuador. Biogeochemistry 77 (1), 57–89. https://doi.org/10.1007/s10533-005-1061-1.

Goodale, C.L., Aber, J.D., McDowell, W.H., 2000. The long-term effects of disturbance on organic and inorganic nitrogen export in the White Mountains,New Hampshire. Ecosystems 3 (5), 433–450. https://doi.org/10.1007/s100210000039.

Hopkins, K.G., Loper, J.V., Craig, L.S., Noe, G.B., Hogan, D.M., 2017. Comparison of sediment and nutrient export and runoff characteristics from watersheds with centralized versus distributed stormwater management. J. Environ. Manag. 203, 286–298. https://doi.org/10.1016/j.jenvman.2017.07.067.

Huang, J.C., Lee, T.Y., Kao, S.J., Hsu, S.C., Lin, H.J., Peng, T.R., 2012. Land use effect and hydrological control on nitrate yield in subtropical mountainous watersheds. Hydrol. Earth Syst. Sci. 16 (3), 699–714. https://doi.org/10.5194/hess-16-699-2012.

Hung, J.J., Yang, C.Y., Lai, I.J., Li, Y.H., 2020. Rainfall and human impacts on weathering rates and carbon-nutrient yields in the watershed of a small mountainous river (Kaoping) in southwestern Taiwan. Sustainability (Switzerland) 12 (18). https://doi.org/10.3390/su12187689.

Hungerbühler, D., Steinmann, M., Winkler, W., Seward, D., Egüez, A., Peterson, D.E., Helg, U., Hammer, C., 2002. Neogene stratigraphy and Andean geodynamics of southern Ecuador. Earth Sci. Rev. 57 (1–2), 75–124. https://doi.org/10.1016/S0012-8252(01)00071-X.

Johnson, A.H., 1979. Estimating solute transport in streams from grab samples. Water Resour. Res. 15 (5).
Kaushal, S.S., Duan, S., Doody, T.R., Haq, S., Smith, R.M., Newcomer Johnson, T.A., Newcomb, K.D., Gorman, J., Bowman, N., Mayer, P.M., Wood, K.L., Belt, K.T., Stack, W.P., 2017. Human-accelerated weathering increases salinization, major ions, and alkalinization in fresh water across land use. Appl. Geochem. 83, 121–135. https://doi.org/10.1016/j.apgeochem.2017.02.006.
Kirchner, J.W., Feng, X., Neal, C., Robson, A.J., 2004. The fine structure of water-quality dynamics: the (high-frequency) wave of the future. Hydrol. Process. 18 (7), 1353–1359. https://doi.org/10.1002/hyp.5537.
Knapp, J.L.A., Von Freyberg, J., Studer, B., Kiewiet, L., Kirchner, J.W., 2020. Concentration-discharge relationships vary among hydrological events, reflecting differences in event characteristics. Hydrol. Earth Syst. Sci. 24 (5), 2561–2576. https://doi.org/10.5194/hess-24-2561-2020.
Knorr, K.H., 2013. DOC-dynamics in a small headwater catchment as driven by redox fluctuations and hydrological flow paths - are DOC exports mediated by iron reduction/oxidation cycles? Biogeosciences 10 (2), 891–904. https://doi.org/10.5194/bg-10-891-2013.
Kortelainen, P., Mattsson, T., Finér, L., Ahtiainen, M., Saukkonen, S., Sallantaus, T., 2006. Controls on the export of C, N, P and fe from undisturbed boreal catchments,Finland. Aquat. Sci. 68 (4), 453–468. https://doi.org/10.1007/s00027-006-0833-6.
Lazo, P.X., Mosquera, G.M., McDonnell, J.J., Crespo, P., 2019. The role of vegetation, soils, and precipitation on water storage and hydrological services in Andean Páramo catchments. J. Hydrol. 572 (March), 805–819. https://doi.org/10.1016/j.jhydrol.2019.03.050.
Lindberg, S.E., Turner, R.R., 1988. Factors influencing atmospheric deposition, stream export, and landscape accumulation of trace metals in forested watersheds. Water Air Soil Pollut. 39 (1–2), 123–156. https://doi.org/10.1007/BF00250954.
Ma, X., Liu, G., Wu, X., Smoak, J.M., Ye, L., Xu, H., Zhao, L., Ding, Y., 2018. Influence of land cover on riverine dissolved organic carbon concentrations and export in the Three Rivers Headwater Region of the Qinghai-Tibetan Plateau. Sci. Total Environ. 630, 314–322. https://doi.org/10.1016/j.scitotenv.2018.02.152.
McDowell, W.H., Asbury, C.E., 1994. Export of carbon, nitrogen, and major ions from three tropical montane watersheds. Limnol. Oceanogr. 39, 111–125.
McDowell, W.H., Lugo, A.E., James, A., 1995. Export of nutrients and major ions from Caribbean catchments. J. N. Am. Benthol. Soc. 14 (1), 12–20. https://doi.org/10.2307/1467721.
Moatar, F., Abbott, B.W., Minaudo, F., Curie, F., Pinay, G., 2017. Elemental properties, hydrology, and biology interact to shape concentration-discharge curves for carbon, nutrients, sediment, and major ions. Water Resour. Res. 53 (2), 1270–1287. https://doi.org/10.1002/2016WR019635.
Moatar, F., Meybeck, M., Raymond, S., Birgand, F., Curie, F., 2012. River flux uncertainties predicted by hydrological variability and riverine material behaviour. Hydrol. Process. 27 (25), 3535–3546. https://doi.org/10.1002/hyp.9464.
Möller, A., Kaiser, K., Guggenberger, G., 2005. Dissolved organic carbon and nitrogen in precipitation, throughfall, soil solution, and stream water of the tropical highlands in northern Thailand. J. Plant Nutr. Soil Sci. 168 (5), 649–659. https://doi.org/10.1002/jpln.200521804.
Mosquera, G., Córdova, M., Célleri, R., 2016. Field Guide and Research Results Ecohydrological Observatories in High – Elevation Tropical Ecosystems. AGU, Chapman Conference, Emerging Issues in Tropical Ecohydrology, June, 8.
Mosquera, G., Lazo, P., Célleri, R., Wilcox, B.P., Crespo, P., 2015. Runoff from tropical alpine grasslands increases with areal extent of wetlands. Catena 125, 120–128. https://doi.org/10.1016/j.catena.2014.10.010.
Musolff, A., Schmidt, C., Selle, B., Fleckenstein, J.H., 2015. Catchment controls on solute export. Adv. Water Resour. 86, 133–146. https://doi.org/10.1016/j.advwatres.2015.09.026.
Padrón, R.S., Wilcox, B.P., Crespo, P., Célleri, R., 2015. Rainfall in the Andean Páramo: new insights from high-resolution monitoring in southern Ecuador. J. Hydrometeorol. 16 (3), 985–996. https://doi.org/10.1175/jhm-d-14-0135.1.
Pesántez, J., Birkel, C., Mosquera, G.M., Peña, P., Arízaga-Idrovo, V., Mora, E., McDowell, W.H., Crespo, P., 2021. High-frequency multi-solute calibration using an in situ UV-visible sensor. Hydrol. Process. 35 (9), e14357 15.
Pesántez, J., Mosquera, G.M., Crespo, P., Breuer, L., Windhorst, D., 2018. Effect of land cover and hydro-meteorological controls on soil water DOC concentrations in a high-elevation tropical environment. Hydrol. Process. 32 (17), 2624–2635. https://doi.org/10.1002/hyp.13224.
Piazza, G.A., Dupas, R., Gascuel-Odoux, C., Grimaldi, C., Pinheiro, A., Kaufmann, V., 2018. Influence of hydroclimatic variations on solute concentration dynamics in nested subtropical catchments with heterogeneous landscapes. Sci. Total Environ. 635, 1091–1101. https://doi.org/10.1016/j.scitotenv.2018.03.394.
Pratt, W.T., Figueroa, J.F., Flores, B.G., 1997. Geology and Mineralization of the Area Between 3 and 48S. Western Cordillera, Ecuador, Open File Report, WCr97r28. British Geological Survey.
Qafoku, N.P., 2015. Climate-change effects on soils: accelerated weathering, soil carbon, and elemental cycling. Advances in Agronomyvol. 131. Elsevier Ltd. https://doi.org/10.1016/bs.agron.2014.12.002.
Quichimbo, P., Tenorio, G., Borja, P., Cárdenas, I., Crespo, P., Célleri, R., 2012. Efectos sobre las propiedades físicas y químicas de los suelos por el cambio de la cobertura vegetal y uso del suelo: páramo de Quimsacocha al Sur del Ecuador. Suelos Ecuatoriales 42 (2), 138–153.
R Core Team, 2019. R: A Language and Environment for Statistical Computing. https://www.r-project.org/.
Resongles, E., Casiot, C., Freydier, R., Gall, M.Le, Elbaz-poulichet, F., 2015. Variation of dissolved and particulate metal (loid) (As, Cd, Pb, Sb, Tl, Zn) concentrations under varying discharge during a Mediterranean flood in a former mining watershed, the Gardon River (France). J. Geochem. Explor. https://doi.org/10.1016/j.gexplo.2015.07.010.
Reynolds, B., Fowler, D., Smith, R.I., Hall, J.R., 1997. Atmospheric inputs and catchment solute fluxes for major ions in five Welsh upland catchments. J. Hydrol. 194 (1–4), 305–329. https://doi.org/10.1016/S0022-1694(96)03226-X.
Ribatet, M., Dutang, C., 2018. {POT}: Generalized Pareto Distribution and Peaks Over Threshold. https://cran.r-project.org/package=POT.
Ritson, J.P., Croft, J.K., Clark, J.M., Brazier, R.E., Templeton, M.R., Smith, D., Graham, N.J.D., 2019. Sources of dissolved organic carbon (DOC) in a mixed land use catchment (Exe, UK). Sci. Total Environ. 666, 165–175. https://doi.org/10.1016/j.scitotenv.2019.02.228.
Roussiez, V., Probst, A., Probst, J.L., 2013. Significance of floods in metal dynamics and export in a small agricultural catchment. J. Hydrol. 499, 71–81. https://doi.org/10.1016/j.jhydrol.2013.06.013.
Salmon, C.D., Walter, M.T., Hedin, L.O., Brown, M.G., 2001. Hydrological controls on chemical export from an undisturbed old-growth Chilean forest. J. Hydrol. 253 (1–4), 69–80. https://doi.org/10.1016/S0022-1694(01)00447-4.
Sánchez-Murillo, R., Romero-Esquivel, L.G., Jiménez-Antillón, J., Salas-Navarro, J., Corrales-Salazar, L., Álvarez-Carvajal, J., 2019. DOC transport and export in a dynamic tropical catchment. J. Geophys. Res. Biogeosci. (June), 2014–2019 https://doi.org/10.1029/2018JG004897.
Schleppi, P., Waldner, P.A., Stähli, M., 2006. Errors of flux integration methods for solutes in grab samples of runoff water, as compared to flow-proportional sampling. J. Hydrol. 319 (1–4), 266–281. https://doi.org/10.1016/j.jhydrol.2005.06.034.
Schmitt, S.R., Riveros-Iregui, D.A., Hu, J., 2018. The role of fog, orography, and seasonality on precipitation in a semiarid, tropical island. Hydrol. Process. 32 (18), 2792–2805. https://doi.org/10.1002/hyp.13228.
Seminario, S., 2016. Incertidumbre en la precipitación espacial diaria causada por Redes Pluviográficas dispersas en una Microcuenca de Páramo densamente monitoreada. Universidad de Cuenca.
Shanley, J.B., McDowell, W.H., Stallard, R.F., 2011. Long-term patterns and short-term dynamics of stream solutes and suspended sediment in a rapidly weathering tropical watershed. Water Resour. Res. 47, 1–11. https://doi.org/10.1029/2010WR009788.
Shih, Y.T., Lee, T.Y., Huang, J.C., Kao, S.J., Chang, 2016. Apportioning riverine DIN load to export coefficients of land uses in an urbanized watershed. Sci. Total Environ. 560–561, 1–11. https://doi.org/10.1016/j.scitotenv.2016.04.055.
Soil Survey Staff, 2003. Keys to soil taxonomy. Change. USDA - NRCS https://doi.org/10.1109/TIP.2005.854494.
Stallard, R.F., Murphy, S.F., 2014. A unified assessment of hydrologic and biogeochemical responses in research watersheds in Eastern Puerto Rico using runoff-concentration relations. Aquat. Geochem. 20 (2–3), 115–139. https://doi.org/10.1007/s10498-013-9216-5.
Sucozhañay, A., Célleri, R., 2018. Impact of rain gauges distribution on the runoff simulation of a small mountain catchment in Southern Ecuador. Water (Switzerland) 10 (9). https://doi.org/10.3390/w10091169.
Swistock, B.R., Edwards, P.J., Wood, F., Dewalle, D.R., 1997. Comparison of methods for calculating annual solute exports from six forested Appalachian watersheds. Hydrol. Process. 11 (7), 655–669. https://doi.org/10.1002/(SICI)1099-1085(199706)11:7<655::AID-HYP525>3.0.CO;2-4.
Tang, J.L., Zhang, B., Gao, C., Zepp, H., 2008. Hydrological pathway and source area of nutrient losses identified by a multi-scale monitoring in an agricultural catchment. Catena 72 (3), 374–385. https://doi.org/10.1016/j.catena.2007.07.004.
Turner, B.F., White, A.F., Brantley, S.L., 2010. Effects of temperature on silicate weathering: solute fluxes and chemical weathering in a temperate rain forest watershed, Jamieson Creek,British Columbia. Chem. Geol. 269 (1–2), 62–78. https://doi.org/10.1016/j.chemgeo.2009.09.005.
United States Bureau of Reclamation, 2001. Water Measurement Manual: A Guide to Effective Water Measurement Practices for Better Water Management. http://www.usbr.gov/pmts/hydraulics_lab/pubs/wmm/.
Vuille, M., Bradley, R.S., Keimig, F., 2000. Climate variability in the Andes of Ecuador and its relation to tropical Pacific and Atlantic Sea Surface temperature anomalies. J. Clim. 13 (14), 2520–2535. https://doi.org/10.1175/1520-0442(2000)013<2520:CVITAO>2.0.CO;2.
Vuorenmaa, J., Rekolainen, S., Lepisto, K., Kenttamies, K., Kauppila, P., 2002. Losses of nitrogen and phosphorus from agricultural and forest areas in Finland during the 1980s and 1990s. Environ. Monit. Assess. 213–248.
Walling, D.E., Webb, B.W., 1985. Estimating the discharge of contaminants to coastal waters by rivers: some cautionary comments. Mar. Pollut. Bull. 16 (12), 488–492.
Wilcke, W., Velescu, A., Leimer, S., Valarezo, C., 2020. Water and nutrient budgets of organic layers and mineral topsoils under tropical montane forest in Ecuador in response to 15 years of environmental change. Forest-Water Interactions. Springer, pp. 565–586 https://doi.org/10.1007/978-3-030-26086-6_11.
Wilcke, Wolfgang, Yasin, S., Valarezo, C., Zech, W., 2001. Change in water quality during the passage through a tropical montane rain forest in Ecuador. Biogeochemistry 55 (1), 45–72. https://doi.org/10.1023/A:1010631407270.
Wymore, A.S., Brereton, R.L., Ibarra, D.E., Maher, K., McDowell, W.H., 2017. Critical zone structure controls concentration-discharge relationships and solute generation in forested tropical montane watersheds. Water Resour. Res., 6279–6295 https://doi.org/10.1002/2016WR020016.Received.
Xue, H., Sigg, L., Gächter, R., 2000. Transport of Cu, Zn and Cd in a small agricultural catchment. Water Res. 34 (9), 2558–2568. https://doi.org/10.1016/S0043-1354(00)00015-4.